



EEG/PPG effective connectivity fusion for analyzing deception in interview

Marzieh Daneshi Kohan¹ · Ali Motie Nasrabadi² · Mohammad Bagher Shamsollahi³ · Ali Sharif⁴

Received: 4 July 2019 / Revised: 13 November 2019 / Accepted: 18 December 2019
© Springer-Verlag London Ltd., part of Springer Nature 2020

Abstract

In this research, the interaction between electroencephalogram (EEG) and, a cardiac parameter, photoplethysmogram (PPG), using connectivity measures to emphasize the importance of autonomic nervous system over the central nervous system during a deception is investigated. In this survey, connectivity analysis was applied, since it can provide information flow of brain regions; moreover, lying and truth appear to be cohered with the flow of information in the brain. Initially, a new wavelet-based approach for EEG/PPG effective connectivity fusion was introduced; then, it was validated for 41 subjects. For each subject, after extracting specific wavelet component of EEG and PPG signals, an effective connectivity network was generated by a generalized partial direct coherence and a direct directed transfer function. The results showed that grand average connectivity patterns were different in some regions for guilty and innocent subjects. The classification results demonstrated that lying could be discriminated from truth with the average accuracy of 84.14% by the leave-one-subject-out method. The present results contribute new information about coupling between EEG and PPG signals.

Keywords Electroencephalogram · Deception detection photoplethysmogram · Effective connectivity · Wavelet · Classification

1 Introduction

Over the past two decades, lie detection methods such as classic polygraph [1–3], thermal imaging [4, 5] and EEG [6–8] have been vigorously developed. In contrast to the polygraph that measures deception's physiological signs and might be confrontable, EEG directly measures deceptive activities from its source and can be less confrontable. Also, thermal imaging is an expensive non-contact technology, which requires complicated calibration despite its advantages. Therefore, the use of less cost and more accessible EEG recording systems was preferred for our research. In this

study, we also used an interview protocol to identify subjects. By definition, interview is a conversation in which questions are asked to elicit concealed information. So, participants were interviewed, answering truthfully or deceptively about their identities at two sessions. The advantages of this protocol were to be more facilitated designs and closer to reality as compared to any other specific protocols used in neurocognitive studies of deception such as GKT¹/CIT² [9].

To analyze our data, we used effective connectivity, which can show dynamic information flow of brain regions and effects of brain regions on each other. Effective/functional connectivity analysis has been widely used in brain analysis of deception [10–13]; hence, it was expected to provide valuable information about deception. In an under-review paper [14], we worked on functional, effective connectivity analysis of brain regions, but in this research, we investigated the interaction between EEG and PPG using connectivity measures to emphasize the importance of autonomic nervous system and their effectiveness of central nervous system during deception.

In some connectivity researches, several methods have been presented on fusion analysis of EEG with HRV (heart

✉ Ali Motie Nasrabadi
nasrabadi@shahed.ac.ir

¹ Department of Biomedical Engineering, Science and Research Branch, Islamic Azad University, Tehran, Iran

² Department of Biomedical Engineering, Shahed University, Tehran, Iran

³ Department of Electrical Engineering, Sharif University of Technology, Tehran, Iran

⁴ Department of Signal Processing, Research Center for Development of Advanced Technologies, Tehran, Iran

¹ Guilty Knowledge Test.

² Concealed Information Test.

Table 1 Review articles on fusion signals for different tasks

	Article ref number	Signals	Integration method	Task
Type 1	[15]	Effective connectivity of EEG, behavior	Regression	Game
	[16]	Functional connectivity of EEG, HRV	Correlation	Resting state
Type 2	[17]	FFT of EEG, HRV	Coherence	Sleep
	[18]	Heart coherence, EEG	Regression	Meditation
	[19]	IMF of EEG, HRV	Coherence	Seizure

In type 1 articles, connectivity of EEG was correlated or regressed with another parameter as behavior or HRV, but in type 2 articles, coherence or regression of EEG was computed with a different parameter. In fact, in type 2 articles, they extracted parameters from EEG or HRV, and then, they computed connectivity between them

rate variability) or behavior signals for different tasks. Antony et al. [15] presented a new method linking neural connectivity to behavioral fluctuations, “behavior-regressed connectivity.” They aimed to understand dynamic connectivity of EEG and transient behavior. They considered behavior measures such as response time as a time series and linked them to the associated time series of brain connectivity with regression to track behavioral fluctuations. Also, the association between heart rate variability and fluctuations in resting-state functional connectivity was investigated by Chang et al. [16]. In addition, dynamic interactions between the spectral power bands of sleep EEG and the HF or LF bands of HRV in healthy young men with coherence were investigated by Jurysta et al. [17]. Correlations between heart rate coherence and EEG variables at baseline and during meditation were also investigated in [18]. We can also mention time-variant coherence analysis between HRV and the channel-related envelopes of adaptively selected EEG components was applied as an indicator for the occurrence of couplings between the central autonomic network (CAN) and the epileptic network before, during and after epileptic seizures in [19].

In order to summarize these articles, we group them in Table 1. As seen, EEG connectivity coupling studies were mostly related to sleep, seizure, rest or meditation researches, and no article has not been presenting a method of integrating EEG and PPG using connectivity in deception detection.

The initial idea came from Antony’s suggestion [15], demonstrating that behavioral metric could be replaced with a physiological measure such as heart rate or blink rate. Since coupling studies can analyze interactions between two phenomena, this study is sought to a better understanding of the physiological mechanisms underlying the interactions between brain dynamic activity and a cardiac parameter during deception. Since no article has been presenting in EEG/PPG connectivity fusion for deception detection so far, it can be a good foundation for future studies. We begin by presenting our experiment, data recording and preprocessing. In section III, we present details of processing of recorded signals. Finally, we present the results in section IV.

2 Method

2.1 Participants

A total of 41 healthy male subjects ranging between the age of 20–34 years [mean age \pm standard deviation (SD): 23.7 ± 1.72 years] with no history of neurological or psychiatric disease participated voluntarily in the experiment. All of volunteers were students or graduated of at minimum bachelor degree. The participants were paid a reward for the participation. After a complete description of the study provided to the participants, written informed consent was obtained. Data were collected in National Brain Mapping Laboratory (NBML) of Iran. This study was approved by the Ethical Committee of the Iran University of Medical Science (number: IR.IUMS.REC.1396.930140180).

2.2 Instruments

EEG signals were recorded using a 32-channel Electrocap according to the 10–20 international system. All active electrodes were referenced to linked ear lobes, with a ground electrode placed on AFZ. Electrode impedance was maintained at below 5 k Ω . Data recording was performed using a g.tec amplifier with 32 channels and g. Recorder software (g.tec, version 2016, Austria). The EEG data were digitized at 512 Hz. To monitor autonomic nervous system (ANS) activity simultaneously by the EEG data, a photoplethysmographic sensor was attached over the index finger of the right hand by means of a flexible Velcro strap. Although newer technologies have been introduced in this field [20–22], this photoelectric pulse sensor provides a clear analog pulse wave signal, which is typically used in lie detection studies [23]. A piezo-electric snoring sensor was also placed on the neck in order to record the voice synchronously; also, to check the process and monitor the movements of subjects, interview was recorded by a webcam.

2.3 Experimental design and procedures

In the first stage, a biography and entertainment form (in Persian language) were filled in. Next, participants in the interview procedure were instructed. We used a deception scenario introduced by Rajoub [4] since it was closer to the reality.

The test was conducted by two sessions; a “true” and a “lie” session. During the true session, participants were required to give accurate, honest responses to all questions about autobiography. During the lie session, the participants were required to give predetermined responses to all questions; in fact, the facilitator set a fake profile with participants and allowed them 10 min to practice it before the interview. The participants were told that they are being to be tested on interviewing skills and that the skill under examination is deception as part of human communications. The facilitator explained to the participants how the examination will be conducted, and they will be rewarded if they are able to convince the examiner of being honest.

Sequence of sessions (i.e., which role plays first) had been arranged randomly for each subject (21 subjects picked lie for the first session and 20 subjects picked truth). In one session, the questions were asked from the candidate’s own profile. In the other, the candidates were asked to study the fake profile. After attaching electrodes and once the subject was ready to examine, the interviewer asked the participant four baseline questions which were answered truthfully to remove the test entrance stress. The interviewer was a psychiatrist and was ignorant of subject’s role in any session (i.e., we had a blind study). Each session consisted of fifteen main questions including three types of neutral, lie/truth and descriptive lie/truth questions. To describe more and off-hand, the interviewer asked some new questions which did not exist in the character profile, e.g., “describe the place where your parents were born.” Two sessions were separated by a 5-min break. At the end of the interview, the facilitator verified by the participants completed the task successfully.

Examples of the main questions used in our experiment are as the followings:

1. How old are you?
2. What is your occupation?
3. Where were you born?
4. What are your hobbies?

Names and surnames of the participants were actual in both sessions and did not change. The interviewer asked this item as a neutral question for both sessions.

2.4 Data preprocessing

The EEG data were processed using EEGLAB functions (version 14.1.1; Delorme & Makeig, 2004) running on

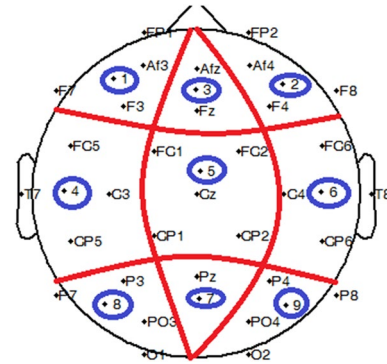


Fig. 1 Regions were considered for analysis: The average of channels of each region was considered as one numbered region

MATLAB 2013a. The raw EEG signals were first high-pass-filtered above 1 Hz and were filtered later with Clean-Line plugin to remove line noise; then, Artifact Subspace Reconstruction (ASR) plugin originally developed by Kothe [24] was used to remove noisy signals automatically. This algorithm removes non-stationary high variance signals from EEG and reconstructs the missing data using a spatial mixing matrix.

Later, removed channels were interpolated through channels around it. The preprocessed EEG data were re-referenced to common average and then decomposed using the independent component analysis (ICA). After using this algorithm, eye blinks and muscles artifact were identified by brain-related independent components (ICs) and manually removed based on their spectra, scalp maps and time courses. Later, the equivalent dipole source localization of these ICs was computed using DIPFIT plugin in EEGLAB. Template 10–20 scalp electrode positions were co-registered in a standard_BESA template brain, using nonlinear warping. A four-shell boundary element method head model based on BESA brain template was used to find the best-fitting equivalent current dipole for each IC. After autofitting dipoles and plotting them, bad components were removed manually again if necessary. Due to the lack of enough data to fit a model for analyzing source information flow dynamics, we divided the head to nine regions, and then, the average of some channels was assigned to one region. Regions which are considered for analysis are shown in Fig. 1. The location of numbered regions is approximate in the following figure.

The PPG signals were prepared for the next step using a band-pass filter with 0.0035–0.18 Hz, detrending and normalization.

2.5 EEG/PPG connectivity fusion analysis

The block diagram of analysis is shown in Fig. 2. We present a new method using wavelet technique for EEG/PPG fusion through connectivity analysis in low-frequency bands in this

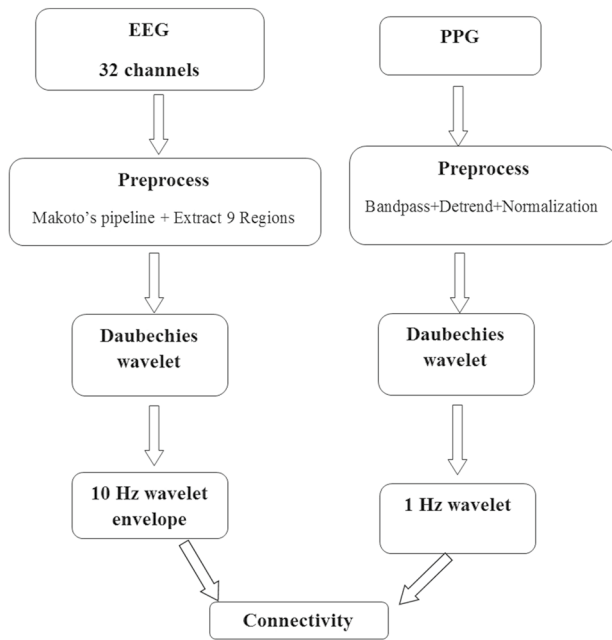


Fig. 2 Block diagram of connectivity analysis; after applying Daubechies 2 wavelet on preprocessed signals, related components were extracted for connectivity analysis

part. Since dynamic of two signals is different, here is how we have solved this problem. After preprocessing input signals, we apply Daubechies 2 wavelet on them. As seen in Figs. 3 and 4, we finally extract upper envelope of 10-Hz wavelet component of EEG and 1-Hz wavelet component of PPG, respectively. This is our idea for EEG/PPG fusion through connectivity analysis, and in this way, we could take down the low-frequency components of the signal by wavelet and could equalize dynamic of two different signals approximately.

For an EEG sample with a 1000-s window, 10-Hz wavelet component of EEG and upper envelope of the wavelet component are shown in Fig. 3; thus, the signal rate was reduced and fitted for fusion with PPG.

A PPG signal sample and 1-Hz wavelet component of PPG are given in Fig. 4.

SIFT data-processing pipeline (an open-source MATLAB toolbox for analysis and visualization of multivariate information flow) was used in the connectivity analysis part. In this step, a multivariate autoregressive (MVAR) model should be fit to the data. A number of algorithms have been proposed to fit VAR models to non-stationary series. For our data, ARfit was chosen.

After fitting the model, two types of connectivities, direct directed transfer function (dDTF) and generalized partial direct coherence (gPDC) between ten achieved channels (nine brain channels and one PPG channel) were computed for each session of the subject (true/lie). Later, the results were compared

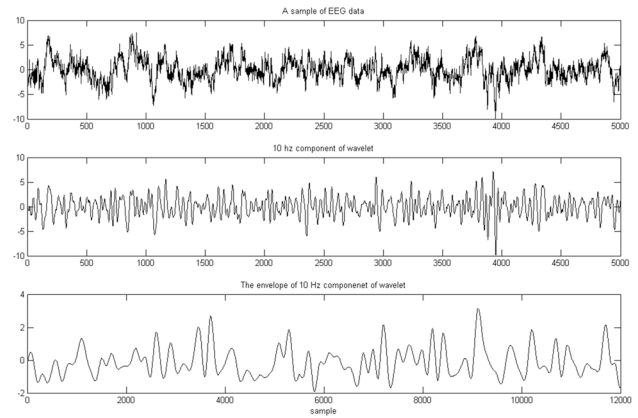


Fig. 3 Raw EEG signal, wavelet component of signal and upper envelope of 10-Hz wavelet component of same EEG are shown from top to down, respectively

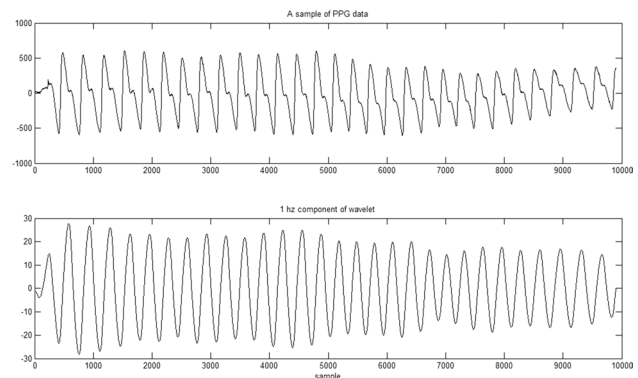


Fig. 4 A PPG sample recorded signal with a sampling rate of 512 Hz is given. As seen in the figure below, 1-Hz wavelet component of PPG sample-extracted signal variations is also well observed

against shuffled surrogate data using a permutation test (100 iterations) and were corrected for multiple comparisons using a false discovery rate (FDR) correction.

2.6 Feature extraction

Deep learning approaches such as convolutional neural networks cannot be used because of insufficient data available, so we used handcrafted extracted features mentioned below.

The size of our connectivity matrices for each subject was $10 \times 10 \times 255 \times 78$ (channel * channel * frequency * number of time windows). We considered ten channels to compute connectivity, nine regions of EEG and one channel of PPG. The features were extracted based on values of connectivities from one channel to another and also from outflow (sum connectivity strengths over outgoing edges) and inflow (sum connectivity strengths over incoming edges) of each channel in each method (dDTF, gPDC). There were two types of analysis based on two feature sets we proposed. For both feature sets, we took the values of connectivity in the average of 1–4 Hz

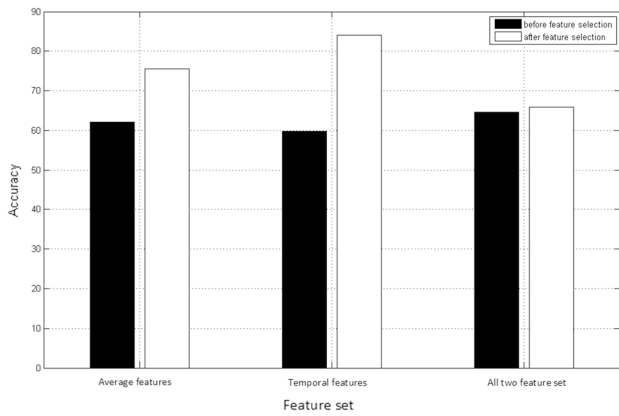


Fig. 5 Accuracy of classifier with temporal, time average and combined feature set before and after feature selection

frequency range for EEG as its envelope of 10-Hz wavelet was near this frequency range, and we had taken the values of connectivity in 1 Hz for PPG.

For the first feature set, called time-average features, we had 10×9 connectivity (except main diagonal) values in the average of 78 available time windows, and for outflow and inflow of each channel, we had $10 + 10$ values. Overall for the first feature set, we owned 220 features for both methods as the input of classifier. For the second feature set, called temporal features, we had $10 \times 9 \times 78$ connectivity (except main diagonal) values along time windows. We did not consider outflow/inflow along time, i.e., we had $10 + 10$ values for outflow and inflow. Overall for the second feature set, we had 14,080 features for both methods as the input of classifier.

3 Results

3.1 Classification results

After normalizing the features, reducing dimension by principal component analysis (PCA) and ranking the top $N/4$ (N is number of all features), a linear discriminant analysis was employed to solve the classification problem. The accuracy for the average of leave-one-subject-out (LOO) using the first feature set was 64.63%. Afterward, to improve the results, we

extracted significant features using feature selection (t test at the $p < 0.05$ level) and the accuracy was 65.85%. The accuracy of the leave-one-subject-out (LOO) average for second feature set was 59.75%/84.14% before/after feature selection, respectively. The accuracy of combining two feature sets was 62.19%/75.60% before/after feature selection, respectively. As seen in Fig. 5, the accuracy of classifier with the temporal feature set was more than the time-average feature set. Also, the accuracy after feature selection was more than before doing that. By combining two feature sets, the accuracy did not improve. Confusion matrix for temporal feature set after feature selection is shown in Table 2.

3.2 Representation of connectivity

Average effective connectivity values of 41 guilty/innocent subjects between nine brain regions by gPDC methods are shown in Tables 3 and 4, respectively, and four of the highest values of connectivities are highlighted for drawing a representation; because of the high numbers of links in the tables, they have refused to draw all of them and have summarized them as representation figures. We ignore the four most values of tables as a pattern for comparing two groups.

A representation of effective connectivity between nine brain regions for average 1–4 Hz for guilty (A) and innocent subjects (B) for gPDC/dDTF methods is shown in Figs. 6 and 7, respectively. As seen effective connectivity pattern of lying has become different only in one region from that of truth-telling. Region 7 (Pz) and its connection with region 3 are merely seen in the guilty group. The activity of this region during deception was also seen in our under-review paper [14]. In addition to being higher values of connectivities in the guilty group than in the innocent group as seen in Fig. 6, we have some distinct links, 7–3 and 2–3 in guilties and 1–3 and 3–2 in innocents. According to dDTF method, in addition to being higher values of connectivities in the guilty group than in the innocent group, we have two distinct links, 7–3 in guilties and 3–1 in innocents (see Fig. 7). The activity of the frontal lobe in both groups indicates mental involvement and decision making, which is more likely to be seen in the guilty group, and according to many articles, the role of the frontal lobe in reasoning and decision making has been confirmed [25, 26].

Table 2 Confusion matrix for average of LOO with significant temporal feature set

Confusion matrix	Actual condition					
	Positive	Negative				
Predicted condition	Positive	TP = 41	FP = 0	Precision = 100%	FDR = 0%	
	Negative	FN = 13	TN = 28	FOR = 31.70%		
		Sensitivity = 75.92%	FPR = 0%	F1-score = 86.31%		
		FNR = 24.07%	Specificity = 100%	Accuracy = 84.14%		

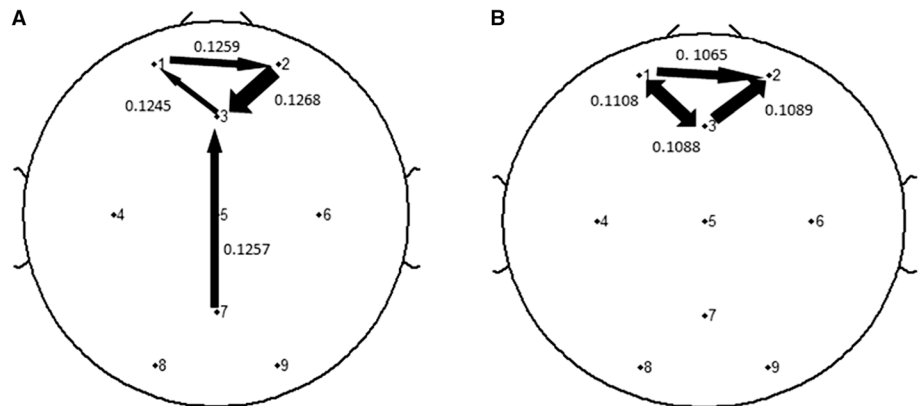
Table 3 Average effective connectivity (gPDC method) values of 41 guilty subjects between nine brain regions and PPG, four of the highest values of connectivities are highlighted as shown in Fig. 6

Guilty group										
GPDC	Reg1	Reg2	Reg3	Reg4	Reg5	Reg6	Reg7	Reg8	Reg9	PPG
Reg1	0.8794	0.1217	0.1245	0.1192	0.1211	0.1193	0.1201	0.1205	0.1229	0.0690
Reg2	0.1259	0.8805	0.1214	0.1181	0.1195	0.1165	0.1205	0.1186	0.1209	0.0694
Reg3	0.1212	0.1268	0.8790	0.1171	0.1178	0.1170	0.1257	0.1217	0.1235	0.0701
Reg4	0.1176	0.1156	0.1199	0.8837	0.1207	0.1191	0.1198	0.1209	0.1186	0.0693
Reg5	0.1199	0.1167	0.1182	0.1201	0.8817	0.1203	0.1183	0.1175	0.1184	0.0685
Reg6	0.1198	0.1187	0.1203	0.1225	0.1214	0.8851	0.1187	0.1184	0.1185	0.0687
Reg7	0.1195	0.1198	0.1224	0.1163	0.1187	0.1169	0.8802	0.1194	0.1181	0.0696
Reg8	0.1182	0.1177	0.1206	0.1214	0.1196	0.1187	0.1217	0.8816	0.1214	0.0675
Reg9	0.1210	0.1232	0.1223	0.1176	0.1195	0.1164	0.1173	0.1200	0.8820	0.0682
PPG	0.1200	0.1186	0.1195	0.1185	0.1202	0.1206	0.1194	0.1191	0.1168	0.9617

Table 4 Average effective connectivity (gPDC method) values of 41 innocent subjects between nine brain regions and PPG; four of the highest values of connectivities are highlighted as shown in Fig. 6

Innocent group										
GPDC	Reg1	Reg2	Reg3	Reg4	Reg5	Reg6	Reg7	Reg8	Reg9	PPG
Reg1	0.9127	0.1037	0.1108	0.1017	0.1033	0.1033	0.1027	0.1025	0.1050	0.0552
Reg2	0.1065	0.9154	0.1089	0.1001	0.1034	0.1013	0.1068	0.0995	0.1044	0.0543
Reg3	0.1088	0.1025	0.9112	0.1027	0.1051	0.1005	0.1052	0.0127	0.1065	0.0538
Reg4	0.1031	0.1018	0.1048	0.9168	0.1038	0.1035	0.0141	0.1044	0.1047	0.0563
Reg5	0.1025	0.1027	0.1043	0.1023	0.9129	0.1027	0.1034	0.1017	0.1012	0.0570
Reg6	0.1023	0.0985	0.1026	0.1035	0.1039	0.9160	0.1036	0.1004	0.1059	0.0536
Reg7	0.1007	0.1035	0.1037	0.0992	0.1058	0.1012	0.9118	0.1056	0.1036	0.0558
Reg8	0.1025	0.1003	0.1027	0.0998	0.1021	0.1002	0.1028	0.9150	0.1037	0.0548
Reg9	0.1019	0.1040	0.1046	0.1018	0.1001	0.1026	0.1033	0.1028	0.9121	0.0556
PPG	0.1065	0.1041	0.1036	0.1055	0.1078	0.1052	0.1045	0.1033	0.1052	0.9777

Fig. 6 A representation of effective connectivity between nine brain regions (gPDC method) for average of 1–4 Hz. **a** The average guilty subjects. **b** The average innocent subjects



The main purpose of this research is to examine EEG/PPG fusion, so we will continue to discuss it. Representations of effective connectivity between nine brain regions (average of 1–4 Hz) and PPG (1 Hz) for guilty (A) and innocent subjects (B) for gPDC/dDTF methods are shown in Figs. 8 and 9, respectively. Three of the highest values of connectivities between EEG regions and PPG are bolded in Tables 3 and 4 as shown in Fig. 8. GPDC results show

that the distinct link is 6 and 4 to PPG for guilty/innocent groups, respectively (see Fig. 8). A dDTF representation show links 7 and 6 to PPG are more active than the others in the guilty group and links 4 and 5 to PPG are more active than the others in the innocent. Therefore, analysis of gPDC and dDTF supports each other, i.e., both showed activity of regions 6 and 4 in lie/truth sessions, respectively. Thus, for both groups, connectivity values of frontal and central lobes

Fig. 7 A representation of effective connectivity between nine brain regions (dDTF method) for average of 1–4 Hz. **a** The average guilty subjects. **b** The average innocent subjects

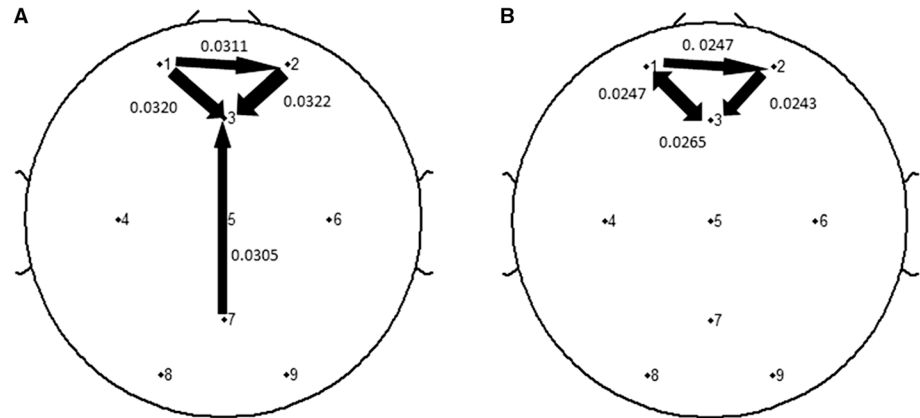


Fig. 8 A representation of effective connectivity between PPG and nine brain regions (GPDC method). **a** The average guilty subjects. **b** The average innocent subjects

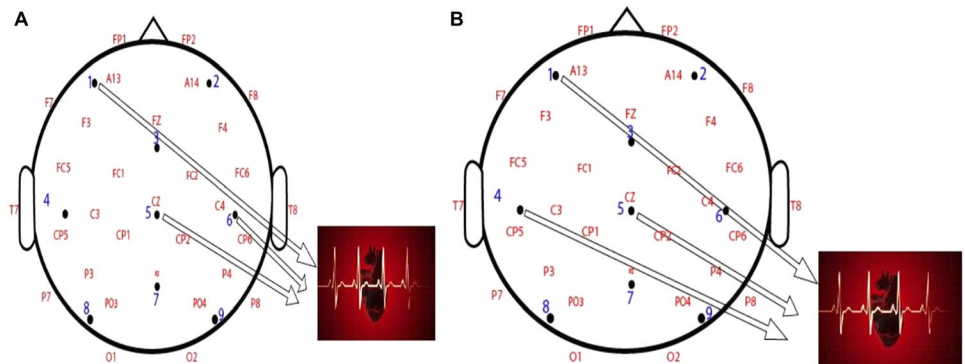
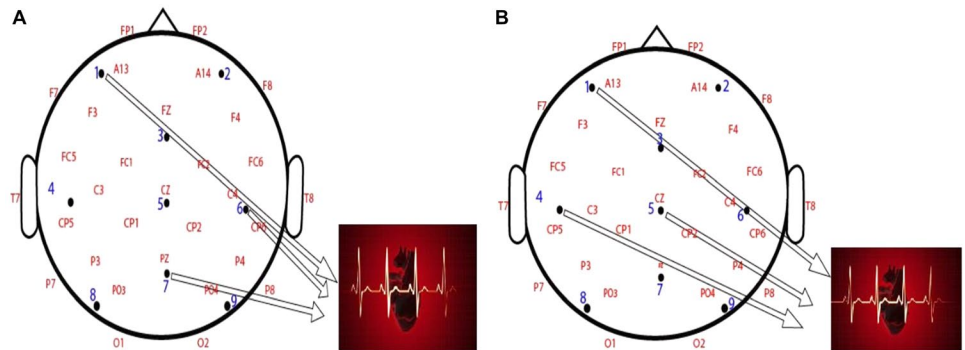


Fig. 9 A representation of effective connectivity between PPG and nine brain regions (dDTF method). **a** The average guilty subjects. **b** The average innocent subjects



with PPG in the guilty group are stronger than innocents. Previous fMRI studies [27, 28] showed that the increased activity in frontal, temporal, limbic lobes and prefrontal cortex could be differentiated lying from truth sessions which our results confirm this.

4 Discussion and conclusions

The present study aims to explore lying about identities by using signal processing methods. It must be stressed that one of the most important purposes of identification is to distinguish the real identities from those of the fake ones. One of the novelties of this paper lies in using an interview-based scenario during EEG recording. The advantages of

this protocol were to be more facilitated and closer to the reality compared to any other specific protocols used in neurocognitive studies of deception such as GKT.

One of our main goals of this research is coupling studies to analyze interactions between two phenomena, so this study is sought to a better understanding of the physiological mechanisms underlying the interactions between brain signals and a cardiac parameter during deception. To analyze our data, we used effective connectivity which can show dynamic information flow of brain regions and effects of brain regions on each other. Since the two heart and brain signals dynamic are different, the current study presents a new method using wavelet technique for EEG/PPG fusion through connectivity analysis in low-frequency bands which may shed new light on integrating EEG and PPG signals

connectivity. As seen in model analysis's section, grand average models of effective connectivity with PPG by gPDC and dDTF methods for average 1–4 Hz of EEG and 1 Hz of PPG were obtained and different models would be achieved for guilty and innocents. High classification accuracies were obtained to test data, strongly supporting the view that is reasonable and feasible to utilize this method in EEG to detect deceptive responses and hence to distinguish guilty from innocent subjects. Our findings showed a significant improvement in accuracies after selecting significant temporal features. By combining two groups of features, accuracy did not improve. Also based on results, values of connectivities in the guilty group were more than innocents, and this is a good parameter to distinguish the two groups. In future works, analysis of connectivity in different frequency ranges can achieve more information about the process of lying.

Acknowledgements I would like to acknowledge National Brain Mapping Laboratory of Iran to provide us with their standard EEG recording system and helping us to collect data.

References

- Matte, J.: *Forensic Psychophysiology Using the Polygraph: Scientific Truth Verification, Lie Detection* (1996)
- Shi, Y., Nguyen, M.H., Blitz, P., French, B., Fisk, S., De la Torre, F., Smailagic, A., Siewiorek, D.P., al' Absi, M., Ertin, E., Kamarck, T., Kumar, S.: Personalized stress detection from physiological measurements. In: *International Symposium on Quality of Life Technology* (2010)
- Karthikeyan, P., Murugappan, M., Yaacob, S.: A review on stress inducement stimuli for assessing human stress using physiological signals. In: *2011 IEEE 7th International Colloquium on Signal Processing and its Applications (CSPA)*. IEEE (2011)
- Rajoub, B.A., et al.: Thermal facial analysis for deception detection. *IEEE Trans. Inf. Forensics Secur.* **9**(6), 1015–1023 (2014). <https://doi.org/10.1109/tifs.2014.2317309>
- Warmelink, L., Vrij, A., Mann, S., Leal, S., Forrester, D., Fisher, R.P.: Thermal imaging as a lie detection tool at airports. *Law Hum. Behav.* **35**(1), 40–48 (2011)
- Abotalebi, V., Moradi, M.H., Khalilzadeh, M.A.: A new approach for EEG feature extraction in P300-based lie detection. *Comput. Methods Progr. Biomed.* **94**, 48–57 (2009). <https://doi.org/10.1016/j.cmpb.2008.10.001>
- Mehrnab, A.H., Nasrabadi, A.M., et al.: A new approach to analyze data from EEG-based concealed face recognition system. *Int. J. Psychophysiol.* **116**, 1–8 (2017). <https://doi.org/10.1016/j.ijpsycho.2017.02.005>
- Ghodousi, M., Nasrabadi, A.M., et al.: Combination of event related potentials and peripheral signals in order to improve the accuracy of the lie detection systems. *JSDP* **12**(2), 73–86 (2015)
- Raskin, D.C., Honts, C.R., Kircher, J.C. (eds.): *Credibility Assessment. Scientific Research and Applications*. Academic Press, Cambridge (2014)
- Davatzikos, C., Ruparel, K., Fan, Y., Shen, D.G., Acharyya, M., Loughhead, J.W., et al.: Classifying spatial patterns of brain activity with machine learning methods: application to lie detection. *NeuroImage* **28**, 663–668 (2005)
- Gao, J., et al.: Exploring time and frequency dependent functional connectivity and brain networks during deception with single-trial event-related potentials. *Sci. Rep.* **6**, 37065 (2016). <https://doi.org/10.1038/srep37065>
- Wang, H., Chang, W., Zhang, C.: Functional brain network and multichannel analysis for the P300-based Brain Computer Interface system of lying detection. *Expert Syst. Appl.* (2016). <https://doi.org/10.1016/j.eswa.2016.01.024>
- Wang, Y., Ng, W.C., Ng, K.S., Yu, K., Wu, T., Li, X.: An Electroencephalography network and connectivity analysis for deception in instructed lying tasks. *PLoS ONE* **10**(2), e0116522 (2015). <https://doi.org/10.1371/journal.pone.0116522>
- Daneshi Kohan, M, et al.: Interview based connectivity analysis of EEG in order to detect deception. *Med. Hypotheses* **136** (2020). <https://doi.org/10.1016/j.mehy.2019.109517>
- Passaro, A.D., et al.: A novel method linking neural connectivity to behavioral fluctuations: behavior-regressed connectivity. *J. Neurosci. Methods* **279**, 60–71 (2017)
- Chang, C., et al.: Association between heart rate variability and fluctuations in resting-state functional connectivity. *NeuroImage* **68**, 93–104 (2013). <https://doi.org/10.1016/j.neuroimage.2012.11.038>
- Jurysta, F., et al.: A study of the dynamic interactions between sleep EEG and heart rate variability in healthy young men. *Clin. Neurophysiol.* **114**, 2146–2155 (2003)
- Kim, D.-K., et al.: Dynamic correlations between heart and brain rhythm during autogenic meditation. *Front. Hum. Neurosci.* **7**, 414 (2013). <https://doi.org/10.3389/fnhum.2013.00414>
- Piper, D., et al.: Time-variant coherence between heart rate variability and EEG activity in epileptic patients: an advanced coupling analysis between physiological networks. *New J. Phys.* **16**, 115012 (2014). <https://doi.org/10.1088/1367-2630/16/11/115012>
- Mazzillo, M., et al.: Characterization of SiPMs with NIR long-pass Interferential and plastic filters. *IEEE Photonics J.* **10**(3), 1–12 (2018). <https://doi.org/10.1109/jphot.2018.2834738>
- Rundo, F., et al.: A nonlinear pattern recognition Pipeline for PPG/ECG medical assessments. In: *Springer Nature, Proceedings of the Fourth National Conference on Sensors*, 21–23 February 2018, Catania, Italy. http://doi.org/10.1007/978-3-030-04324-7_57 (2018)
- Vincenzo, et al.: PPG/ECG multisite Combo system based on SiPM Technology. *Sensors* **353–360**, 2017 (2018). https://doi.org/10.1007/978-3-030-04324-7_44
- Anastasova, K., et al.: Differences in the quality of the photoplethysmograph signal in subjects with and without nail polish. *Eur. Polygraph* **12**(1–43), 7–17 (2018). <https://doi.org/10.2478/ep-2018-0001>
- Mullen, T.R., Kothe, C.A., Chi, Y.M., Ojeda, A., Kerth, T., Makeig, S., Jung, T.P., Cauwenberghs, G.: Real-time neuroimaging and cognitive monitoring using wearable dry EEG. *IEEE Trans. Biomed. Eng.* **62**(11), 2553–2567 (2015). <https://doi.org/10.1109/tbme.2015.2481482>
- Volz, K.G., Schubotz, R.I., Yves von Cramon, D.: Decision making and the frontal lobes. *Curr. Opin. Neurol.* **19**(4), 401–406 (2006). <https://doi.org/10.1097/01.wco.0000236621.83872.71>
- Collins, A., Koechlin, E.: Reasoning, learning, and creativity: frontal lobe function and human decision-making. *PLoS Biol.* **10**(3), e1001293 (2012). <https://doi.org/10.1371/journal.pbio.1001293>
- Peplow, M.: Brain imaging could spot liars. *Nature* (2004). <https://doi.org/10.1038/news041129-1>
- Langleben, D.D., et al.: Brain activity during simulated deception: an event-related functional magnetic resonance study. *NeuroImage* **15**(3), 727–732 (2002)

Publisher's Note Springer Nature remains neutral with regard to jurisdictional claims in published maps and institutional affiliations.